

# The Relaxation Properties of Myofibrils Are Compromised by Amino Acids that Stabilize $\alpha$ -Tropomyosin

Beatrice Scellini,<sup>1</sup> Nicoletta Piroddi,<sup>1</sup> Alexander M. Matyushenko,<sup>2</sup> Dmitrii I. Levitsky,<sup>2</sup> Corrado Poggesi,<sup>1</sup> Sherwin S. Lehrer,<sup>3</sup> and Chiara Tesi<sup>1,\*</sup>

<sup>1</sup>Department of Experimental and Clinical Medicine, University of Florence, Florence, Italy; <sup>2</sup>A.N. Bach Institute of Biochemistry, Research Center of Biotechnology, Russian Academy of Sciences, Moscow, Russia; and <sup>3</sup>Dedham, Massachusetts

**ABSTRACT** We investigated the functional impact of  $\alpha$ -tropomyosin (Tm) substituted with one (D137L) or two (D137L/G126R) stabilizing amino acid substitutions on the mechanical behavior of rabbit psoas skeletal myofibrils by replacing endogenous Tm and troponin (Tn) with recombinant Tm mutants and purified skeletal Tn. Force recordings from myofibrils (15°C) at saturating  $[Ca^{2+}]$  showed that Tm-stabilizing substitutions did not significantly affect the maximal isometric tension and the rates of force activation ( $k_{ACT}$ ) and redevelopment ( $k_{TR}$ ). However, a clear effect was observed on force relaxation: myofibrils with D137L/G126R or D137L Tm showed prolonged durations of the slow phase of relaxation and decreased rates of the fast phase. Both Tm-stabilizing substitutions strongly decreased the slack sarcomere length (SL) at submaximal activating  $[Ca^{2+}]$  and increased the steepness of the SL-passive tension relation. These effects were reversed by addition of 10 mM 2,3-butanedione 2-monoxime. Myofibrils also showed an apparent increase in  $Ca^{2+}$  sensitivity. Measurements of myofibrillar ATPase activity in the absence of  $Ca^{2+}$  showed a significant increase in the presence of these Tms, indicating that single and double stabilizing substitutions compromise the full inhibition of contraction in the relaxed state. These data can be understood with the three-state (blocked-closed-open) theory of muscle regulation, according to which the mutations increase the contribution of the active open state in the absence of  $Ca^{2+}$  ( $M^-$ ). Force measurements on myofibrils substituted with C-terminal truncated TnI showed similar compromised relaxation effects, indicating the importance of TnI-Tm interactions in maintaining the blocked state. It appears that reducing the flexibility of native Tm coiled-coil structure decreases the optimum interactions of the central part of Tm with the C-terminal region of TnI. This results in a shift away from the blocked state, allowing myosin binding and activity in the absence of  $Ca^{2+}$ . This work provides a basis for understanding the effects of disease-producing mutations in muscle proteins.

## INTRODUCTION

Tropomyosin (Tm) is an  $\alpha$ -helical, coiled-coil, actin-binding protein that together with troponin (Tn) regulates the cooperative  $Ca^{2+}$  activation of striated muscle contraction. Adjacent Tm molecules, each covering seven actin monomers and interacting with one Tn (the so-called actin<sub>7</sub>TmTn structural unit), bind head-to-tail and form a continuous strand along the entire length of the actin filament, blocking sites for myosin binding. When  $Ca^{2+}$  binds to Tn, the Tm strand azimuthally moves and permits myosin access on actin and cross-bridge formation (1–3). The different molecular properties of Tm isoforms in vertebrate striated muscle

are involved in the dynamics of  $Ca^{2+}$ -induced Tm movement on actin and the highly cooperative activation of contraction (4,5). The stability of Tm is typical of two-stranded,  $\alpha$ -helical, coiled-coil proteins whose structure consists of repeats of seven amino acid residues ( $a-g$ ) that form a hydrophobic core with residues 1 and 4 ( $a$  and  $d$ ), and is further stabilized by charged interchain interactions between residues 5 and 7 ( $e$  and  $g$ ) and polar interfaces exposed to solvent (residues 2, 3, and 6, or  $b$ ,  $c$ , and  $f$  (6,7)). The modulation of Tm molecular stability by the presence of single or clusters of noncanonical amino acids (e.g., charged amino acids where hydrophobic ones are expected) seems to serve a relevant functional role by imparting a variable degree of mobility to the protein (generally referred to as flexibility). This could strongly impact Tm-Tn interactions,  $Ca^{2+}$  regulation, and myosin cross-bridge formation with actin. Interestingly, cardiomyopathy-linked

Submitted September 1, 2016, and accepted for publication December 8, 2016.

\*Correspondence: [chiara.tesi@unifi.it](mailto:chiara.tesi@unifi.it)

Editor: James Sellers.

<http://dx.doi.org/10.1016/j.bpj.2016.12.013>

© 2016

mutations of Tm have been shown to affect molecular flexibility, leading to the hypothesis that the modification of flexibility could be a key factor in altered  $\text{Ca}^{2+}$  sensitivity and phenotype pathological modifications (8). Among Tm noncanonical amino acids, recent studies have examined two highly conserved residues in the middle part of the  $\alpha\alpha\text{Tm}$  molecule: D137 (a charged residue in a *d* hydrophobic position) and G126 (a small, neutral residue in a *g* charged position). Replacement of these residues with canonical ones, D137L and G126R (9,10), was shown in solution studies to significantly increase coiled-coil stability and decrease molecular mobility or flexibility (9,11–13). A significant decrease in the flexibility of reconstructed thin filaments with the combined D137L/G126R substitution was also shown by means of the two-bead optical trap technique (14).

Interestingly,  $\text{Ca}^{2+}$  regulation dynamics in the intact thin filament are also affected, as shown by measurements of thin-filament-induced activation of S1 ATPase activity in the presence of D137L or G126R  $\alpha\alpha\text{Tm}$  (9,10), and by the maximal sliding velocity of regulated actin filaments in *in vitro* motility assays (15,16). All of these studies reported a clear functional change in the presence of one or both stabilizing substitutions and a generalized increase in apparent  $\text{Ca}^{2+}$  sensitivity. Regarding the functional impact of Tm-stabilizing substitutions in organized sarcomeric systems, little is known. The only available information was obtained by the generation of a transgenic mouse model expressing D137L  $\alpha\alpha\text{Tm}$  (17), which led to a phenotype alteration related to dilated cardiomyopathy and impairment of both *in situ* cardiac function and cardiomyocyte contractility.

Here, we investigated the functional role of Tm flexibility in regulating the thin-filament-mediated activation of muscle contraction by using single skeletal myofibrils, a preparation that allows us to replace endogenous Tm with recombinant forms, as well as to maintain a homogeneous protein composition in terms of posttranslational features (18,19). In particular, the purpose of this work was to determine the functional impact of recombinant  $\alpha\alpha\text{Tm}$  carrying one (D137L) or two (D137L/G126R) substitutions on the mechanical behavior of resting and maximally  $\text{Ca}^{2+}$ -activated rabbit fast skeletal myofibrils, as well as on their ATPase activity in the virtual absence of  $\text{Ca}^{2+}$ . The results showed that both mutants decrease the ability of the thin filament to completely switch off tension in the absence of  $\text{Ca}^{2+}$  without affecting the kinetics and degree of  $\text{Ca}^{2+}$  activation of force generation. The data were very similar to what was observed by replacing cardiac TnI (cTnI) with a C-terminal truncated form of cTnI in skeletal myofibrils. Both sets of data can be explained by the increased contribution of an active open state in the absence of  $\text{Ca}^{2+}$  ( $M^-$  (20)) according to the three-state muscle regulation theory (21). Furthermore, our results support the hypotheses that the local and long-range flexi-

bility of the Tm coiled-coil structure, as well as some interactions of the Tm central part with TnI (2,22) and/or myosin (16), may be crucial to maintain the full inhibition of acto-myosin interactions of the resting state. These results confirm previous preliminary observations in skeletal myofibrils replaced with D137LTm-Tn (23) or for a C-terminal truncated form of cTnI (24).

## MATERIALS AND METHODS

### Proteins

We used recombinant human  $\alpha\alpha\text{Tm}$  (or Tpm1.1 according to (25)) with an Ala-Ser N-terminal extension to imitate naturally occurring N-terminal acetylation of native Tm (26). Human  $\alpha\alpha\text{Tm}$  is almost identical to rabbit  $\alpha\alpha\text{Tm}$  (with only one conservative change, R220K), and N-terminal modification of Tm has been shown to not interfere with the functional properties of *in vitro* (26) and myofibril (27) systems. Also, the three recombinants (control, D137L, and D137L/G126R) included the mutation C190A to prevent air oxidation. As described previously (16), all of these Tm species were overexpressed in BL21(DE3) according to standard methods, extracted by heating, fractionated by reducing the pH to 4.8, and purified by anion exchange chromatography using a HiTrap QXL column. The C190A mutation mimics the reduced state of cysteine in the Tm molecule, which is typical of living muscle (27), and had no appreciable effect on the tryptic digestion of Tm (9) or on its thermal unfolding and domain structure (12). Purified rabbit psoas Tn was kindly provided by Prof. M.A. Geeves (University of Kent, Kent, UK).

### Myofibril experiments: preparation and extraction of endogenous Tm-Tn protein, and reconstitution protocol

Single myofibrils or thin bundles of myofibrils were isolated from fast psoas muscle of rabbits killed by pentobarbital (120 mg/kg) administration through the marginal ear vein in accordance with the official regulations of the European Community Council on the Use of Laboratory Animals (Directive 86/609/EEC) and using protocols approved by the Ethics Committee for Animal Experiments of the University of Florence. After dissection, muscles were cut in strips ~0.5 cm wide, tied at rest length to rigid wood sticks, and stored at  $-20^\circ\text{C}$  for no more than 6 months in a 200 mM ionic strength rigor solution (100 mM KCl, 2 mM  $\text{MgCl}_2$ , 1 mM EGTA, 50 mM Tris, pH 7.0) supplemented with glycerol 50%. Single myofibrils or bundles of two to three myofibrils were prepared by homogenization of glycerinated psoas muscle as previously described (28–30). All solutions were kept at  $\sim 0^\circ\text{C}$  and contained a cocktail of protease inhibitors including 10  $\mu\text{M}$  leupeptin, 5  $\mu\text{M}$  pepstatin A, 200  $\mu\text{M}$  phenyl-methylsulphonylfluoride, 10  $\mu\text{M}$  E64, 500  $\mu\text{M}$  Na $\text{N}_3$  and 500  $\mu\text{M}$  dithiothreitol. In myofibrils, the endogenous regulatory proteins Tm and Tn were extracted and replaced with recombinant human  $\alpha\alpha\text{Tm}$  forms and purified rabbit fast skeletal Tn as previously described (18,27). The recombinant  $\alpha\alpha\text{Tm}$  species replaced in myofibrils were then control, D137L, and D137L/G126R. Briefly, myofibrils were washed by centrifugation (five to seven times) in a mildly alkaline/low-ionic-strength solution (2 mM Tris-HCl, pH 8.0) to remove native Tm and Tn. Extracted myofibrils were then washed in rigor solution and reconstituted with exogenous  $\alpha\alpha\text{Tm}$  (5  $\mu\text{M}$ ) and Tn (2  $\mu\text{M}$ ) in a two-step protocol ( $0^\circ\text{C}$ , 2 h incubation per step). Finally, the reconstituted myofibrils were washed and stored in a 200 mM ionic strength rigor solution at  $4^\circ\text{C}$  and used within 3 days. In some experiments (see Fig. 7), only the Tn complex was replaced with cardiac isoforms, using the procedure and proteins (cTnT, cTnC, and cTnI<sub>1-192</sub>) described in (31). At

each stage of the protocol, samples were retained from both supernatant and pellet fractions for electrophoretic assays. SDS-PAGE gels (12%) were prepared as previously described (31), stained with 0.1% Coomassie blue, scanned, and analyzed using UN-SCAN-IT gel 6.0 software (Silk Scientific, Orem, UT). T<sub>m</sub> extraction and replacement were assessed in each lane by the densitometry ratio of T<sub>m</sub> to the actin band. Although the T<sub>m</sub> and TnT peaks overlapped in gel profiles, peaks of approximately equal intensity were sufficiently separated for quantification. Myofibril preparations that did not show the appropriate gel patterns were discarded. Together with gel analyses of the bulk preparations, the mechanical properties of the myofibrils after T<sub>m</sub>-Tn replacement (maximal calcium-activated force and its kinetics of development and relaxation) were assessed as a key test for the preservation of actin/T<sub>m</sub>/Tn stoichiometry (18,19).

## Apparatus and experimental protocol

Mechanical measurements from T<sub>m</sub>-Tn-replaced myofibrils in isometric conditions were performed during activation-relaxation cycles achieved by fast solution switching as previously described (28–30). For force recording, a small volume of myofibril suspension was transferred to a thermostatically controlled observation chamber mounted on an inverted microscope (15°C). Myofibrils in relaxing solution (pCa 9.0) were mounted horizontally between two glass microtools: one connected to a length-control motor and the other acting as a calibrated cantilevered force probe (2–6 nm/nN; frequency response of 2–5 kHz). After mounting, the initial length of selected preparations (single myofibrils or bundles of a few myofibrils, 25–80 μm long, 1–4 μm wide) was set just 5–10% above the slack length and the initial sarcomere length (SL) was measured. Mounted myofibrils were then continuously perfused by one of two streams of relaxing (pCa 9.0) or activating (pCa 4.5) solution flowing by gravity from a double-barreled glass pipette placed within a 1 mm distance. The solution change, achieved by displacing the perfusion pipette with a stepped-motor-controlled system, occurred with a time constant of 2–4 ms and was complete in <10 ms. The maximal force developed (P<sub>0</sub>) was measured by the deflection of the shadow of the force probe projected on a split photodiode and normalized by the cross-sectional area of the preparation. The rate of force development (*k*<sub>ACT</sub>) and the rate of force redevelopment according to the release-retch protocol (*k*<sub>TR</sub>) (32) were estimated from the time required to reach 50% of the maximal isometric force. The rate constant of the early slow force decline (slow *k*<sub>REL</sub>) was estimated from the slope of the regression line fitted to the tension trace normalized to tension just before relaxation. The duration of the slow relaxation phase was estimated from the start of the solution change. The rate constant for the final fast phase of tension decline (fast *k*<sub>REL</sub>) was estimated from a monoexponential fit (33,34). Resting tension development (RT) at pCa 9.0 was measured by imposing up to 10–20% releases of initial length to myofibrils mounted for force recording. By the same procedure, quasi-steady-state SL-resting tension relations were determined several seconds after the imposition of ramp elongations of different extents (10–30% of the initial myofibril length), when most of the stress relaxation was over. In a few experiments, the Ca<sup>2+</sup> sensitivity of the force development of T<sub>m</sub>-Tn-replaced myofibrils was measured by a Ca<sup>2+</sup>-jump protocol, i.e., by sequentially activating myofibrils at submaximal (pCa 5.95) and maximal (pCa 4.50) Ca<sup>2+</sup> and measuring the ratio of developed force. The diameter, average SL, and length of mounted myofibrils were measured by calibrated visualization of video images.

## Solutions for mechanical experiments

All activating and relaxing solutions were calculated as described previously (30) at pH 7.0 and contained 10 or 1 mM of total EGTA (CaEGTA/EGTA ratio set to obtain different pCa values in the range of 9.00–4.50),

5 mM MgATP, 1 mM free Mg<sup>2+</sup>, 10 mM 3-(N-morpholino) propanesulfonic acid, propionate, and sulfate to adjust the final solution to an ionic strength of 200 mM and a monovalent cation concentration of 155 mM. Creatine phosphate (10 mM) and creatine kinase (200 units/mL<sup>-1</sup>) were added to all solutions to minimize alterations in the concentration of MgATP and its hydrolysis products. Contaminant [Pi] (~170 μM in standard solutions) was reduced to <5 μM (Pi-free solutions) by a Pi-scavenging enzyme system (purine-nucleoside-phosphorylase with substrate 7-methyl-guanosine) (30,35). In a few experiments, 10 mM 2,3-butanedione 2-monoxime (BDM) was added to the relaxing solution. All experimental solutions contained 10 μM leupeptin, cysteine protease inhibitor E-64, and 0.5 mM dithiothreitol. Nucleoside phosphorylase (bacterial), 7-methylguanosine, ATP, BDM, leupeptin, and E-64 were purchased from Sigma-Aldrich (St. Louis, MO). Creatine phosphate and creatine kinase were obtained from Roche Diagnostics (Basel, Switzerland).

## ATP hydrolysis measurements from myofibril suspensions

Steady-state ATP hydrolysis of T<sub>m</sub>-Tn-replaced rabbit psoas myofibrils in relaxing solution was measured using the Malachite Green phosphate assay (BioAssay Systems, Hayward, CA). Briefly, myofibrils subjected to the T<sub>m</sub>-Tn extraction-replacement protocol were washed and resuspended with a modified relaxing solution that did not contain MgATP, protease inhibitors, and creatine phosphate. The concentration of myosin in the suspension was determined spectrophotometrically (36) from the absorbance at 280 nm (BioSpectrometer, Eppendorf, Hamburg, Germany) in 2% SDS, with  $E^{1\%}_{1\text{cm}} = 7$  and assuming that myosin had a molecular mass of  $5 \times 10^5$  D and represented 50% of the total protein content (typically 0.2–0.3 mg/mL (36,37)). The mean head concentration in reaction solution (250 μL) was set at ~0.5 μM. The reaction was started in a constant-temperature bath at 30°C by adding 50 μL of 5 mM MgATP dissolved in the same experimental solution (final concentration 1 mM). The reaction was arrested by acid quench at different times by adding 250 μL of ice-chilled 0.67 M trichloroacetic acid. The phosphate assay was performed by adding 20 μL of Malachite Green reagent to 80 μL of the acid-quenched reaction mixtures and measuring the absorbance at 630 nm after 30 min incubation at room temperature. ATP hydrolysis was expressed as the ratio of [P<sub>i</sub>] to [myosin head] (μM/μM).

## Data acquisition and analysis

Force and length analog signals were continuously monitored throughout the experiments using commercial software and programs (LabVIEW, National Instruments, Austin, TX) modified for our use. The same signals were also recorded during experimental protocols and later used for data analysis. Data measurements were made directly with commercial software (Origin) and an in-house-written LabVIEW analysis program that converted the analog signal to numeric values. The data are expressed and plotted as the mean ± SEM obtained from *n* myofibrils. Differences between the three myofibril groups (control, D137L, and D137L/G126R ααTm) were tested by means of unpaired Student's *t*-tests. A value of *p* < 0.05 was considered statistically significant.

## RESULTS

### Reconstitution of rabbit psoas myofibrils with mutant Tms

The substitution of three different mutant ααTms (control, D137L, and D137L/G126R) for native Tm in myofibrils

was performed by extraction and reconstitution of Tm-Tn in a two-step process, as outlined in [Materials and Methods](#). Samples of all myofibril preparations used for mechanical measurements were retained for SDS-PAGE analysis, as well as native (unextracted) and Tm-Tn-extracted myofibrils. [Fig. 1 A](#) shows a representative electrophoretic gel of samples from D137L Tm-Tn-extracted and -reconstituted myofibrils. The amount of protein loaded (4–10  $\mu\text{g}$ ) in the different lanes differed slightly due to protein loss during the preparation. The degree of Tm extraction and replacement in each lane was quantified from the intensity profiles of scanned gels. The mean data reported in [Fig. 1 B](#) show that after extraction, the Tm/actin ratio of myofibrils dropped from  $0.53 \pm 0.01$  (native) to  $0.11 \pm 0.01$  (extracted) and then almost fully recovered, independently of the recombinant  $\alpha\text{Tm}$  used. These results indicate that  $80\% \pm 1\%$  of Tm was

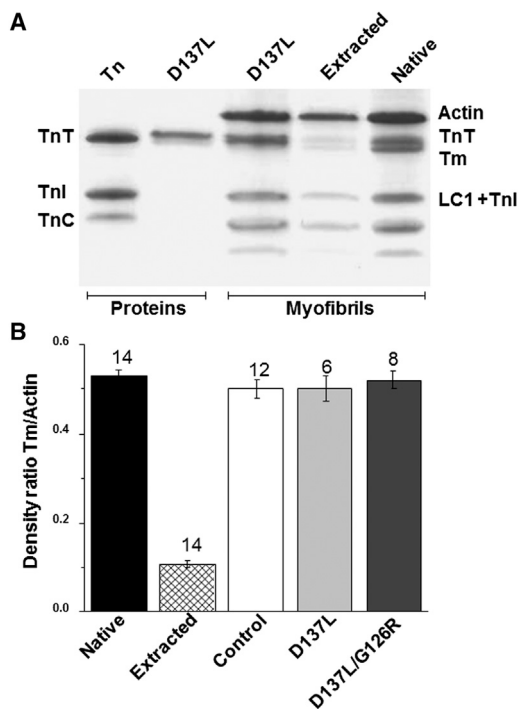


**FIGURE 1** Tm-Tn reconstitution in rabbit skeletal myofibrils. (A) Representative Coomassie blue-stained 12% SDS-PAGE gel image of the extraction and reconstitution of regulatory proteins in rabbit psoas skeletal myofibrils using D137L  $\alpha\text{Tm}$ . Native, extracted, and D137L  $\alpha\text{Tm}$ -Tn-reconstituted myofibrils are shown on the right. A skeletal Tn complex and D137L  $\alpha\text{Tm}$  are shown on the left. (B) Efficiency of extraction-reconstitution with different  $\alpha\text{Tm}$  molecules in rabbit skeletal myofibrils, averaged from a densitometry analysis of SDS-PAGE gels. Myofibrils were extracted and replaced with Tn and control, D137L, or D137L/G126R  $\alpha\text{Tm}$ . Tm band intensities are expressed relative to the corresponding actin band. All values are given as mean  $\pm$  SEM (the number of averaged gels is given above the bars). From the left, Tm/actin density ratios: native,  $0.53 \pm 0.01$ ; extracted,  $0.11 \pm 0.01$ ; control,  $0.50 \pm 0.02$ ; D137L,  $0.50 \pm 0.03$ ; D137L/G126R,  $0.52 \pm 0.02$ .

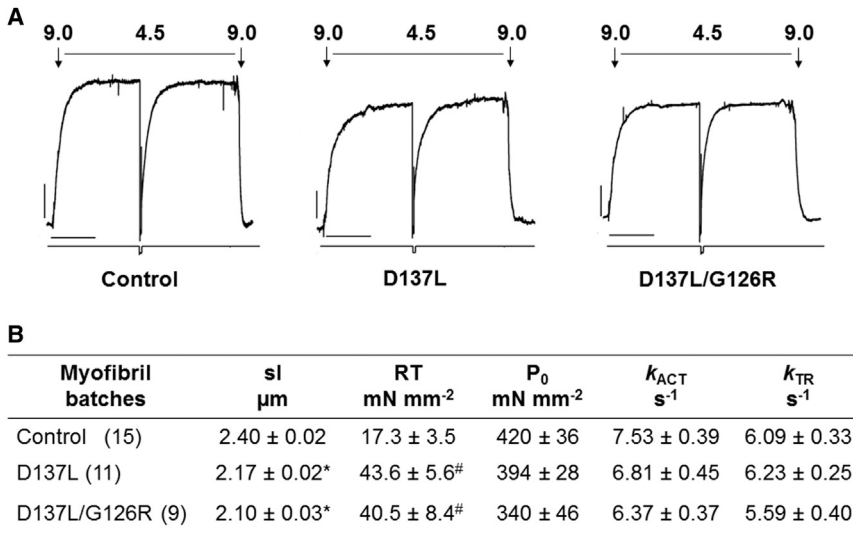
removed and Tm replacement in reconstituted myofibrils attained  $95\% \pm 2\%$ ,  $96\% \pm 2\%$ , and  $97\% \pm 2\%$  with control, D137L, and D137L/G126R, respectively (mean  $\pm$  SEM;  $n = 6$ –14). As expected, extraction/replacement of fast skeletal Tn was 100% (19).

### D137L and D137L/G126R Tms do not affect myofibril activation kinetics and maximal isometric tension, but impair relaxation

Representative mechanical recordings of active force development, force redevelopment, and relaxation of myofibrils reconstituted with control, D137L, and D137L/G126R are shown in [Figs. 2 A](#) and [3 A](#). In each activation (pCa 4.5)-relaxation (pCa 9.0) cycle was performed by fast solution switching, the following data were obtained: 1) maximal steady-state tension ( $P_0$ , force developed at pCa 4.5 normalized over myofibril cross-sectional area); 2) the rate of force development upon maximal  $\text{Ca}^{2+}$  activation ( $k_{\text{ACT}}$ ); and 3) the rate of tension redevelopment upon a rapid 20% release-restretch imposed at maximal activation ( $k_{\text{TR}}$ ). Average values are shown in [Fig. 2 B](#).

The average rates of the slow linear and fast exponential phases of full force relaxation (slow  $k_{\text{REL}}$  and fast  $k_{\text{REL}}$ , respectively), as well as the duration of the slow phase of force relaxation (33), are reported in [Fig. 3, B–D](#). The activation-relaxation traces show that  $\text{Ca}^{2+}$  regulation of contraction is well preserved in myofibrils reconstituted with all of the  $\alpha\text{Tm}$ s used here, with no significant difference in maximal tension, rate of activation ( $k_{\text{ACT}}$ ), or rate of tension redevelopment ( $k_{\text{TR}}$ ). This confirms the effective reconstitution of the exogenous regulatory proteins into the sarcomere after extraction, as already suggested by electrophoretic analysis, and shows that Tms with reduced flexibility do not impair maximal force generation or the kinetics of its development after  $\text{Ca}^{2+}$  activation. However, the force relaxation transients of the mutant myofibrils compared with control myofibrils showed a marked difference, with clearly increased effects associated with the presence of two Tm-stabilizing substitutions (D137L/G126R) compared with one (D137L). As shown in [Fig. 3 A](#), myofibrils reconstituted with D137L/G126R Tm exhibited a markedly prolonged duration of the slow phase of relaxation ([Fig. 3 B](#);  $p < 0.0005$ ) and a significant decrease in the rate of the fast phase of relaxation compared with myofibrils with control Tm ([Fig. 3 D](#);  $p < 0.0005$ ). Smaller but similar effects were observed with D137L Tm. The rate of the slow isometric force decay was unchanged by the mutant Tms ([Fig. 3 C](#)), as expected from previous observations regarding the lack of effect of Tm isoforms (19) or Tm posttranslation modifications (38) on this parameter. Interestingly, the changes in relaxation associated with the presence of these substitutions in the central part of  $\alpha\text{Tm}$  are similar to the





1 s. Control  $\alpha\text{Tm}$ : SL 2.50  $\mu\text{m}$ ,  $P_0$  409  $\text{mN mm}^{-2}$ ,  $k_{\text{ACT}}$  6.7  $\text{s}^{-1}$ ,  $k_{\text{TR}}$  6.2  $\text{s}^{-1}$  D137L  $\alpha\text{Tm}$ : SL 2.31  $\mu\text{m}$ ,  $P_0$  436  $\text{mN mm}^{-2}$ ,  $k_{\text{ACT}}$  6.9  $\text{s}^{-1}$ ,  $k_{\text{TR}}$  6.0  $\text{s}^{-1}$ ; D137L/G126R  $\alpha\text{Tm}$ : SL 2.09  $\mu\text{m}$ ,  $P_0$   $\text{mN mm}^{-2}$ ,  $k_{\text{ACT}}$  6.8  $\text{s}^{-1}$ ,  $k_{\text{TR}}$  6.5  $\text{s}^{-1}$ . (B) Average values of the kinetics and maximal active and resting tensions of rabbit psoas myofibrils reconstituted with recombinant  $\alpha\text{Tm}$  species at 15°C. All values are mean  $\pm$  SEM (pCa 4.5) and each group of data was obtained from different skeletal myofibril batches (numbers in parentheses are the number of myofibrils). \* $p < 0.0001$ , # $p < 0.01$  (Student's  $t$ -test) versus the same parameter measured in control  $\alpha\text{Tm}$ -reconstituted myofibrils.

FIGURE 2 Maximal isometric active tension generation in rabbit psoas myofibrils containing recombinant control, D137L, or D137L/G126R  $\alpha\text{Tm}$  at 15°C. (A) Representative recordings (top traces) of force development of control  $\alpha\text{Tm}$  (left), D137L  $\alpha\text{Tm}$  (middle), and D137L/G126R  $\alpha\text{Tm}$  (right) reconstituted skeletal myofibrils maximally activated (pCa 4.5) and fully relaxed (pCa 9.0) by the fast solution switching technique. Bottom traces show where the rapid release (20%  $I_0$ ) and re-stretch of myofibril length was performed to measure the exponential redevelopment of force ( $k_{\text{TR}}$ ) under steady maximal tension conditions. The rate of tension generation after fast  $\text{Ca}^{2+}$  activation ( $k_{\text{ACT}}$ ) was measured from the kinetics of force development upon solution switching from a relaxing to an activating solution. Bars above the traces correspond to the timing of the solution change, and numbers correspond to pCa values of activating and relaxing solutions. Tension calibration (vertical bar): 100  $\text{mN mm}^{-2}$ ; time calibration (horizontal bar):

relaxation dynamics observed for incomplete/impaired switching-off of the regulatory apparatus of native Tm, as in the case of relaxation from maximal to submaximal activating  $[\text{Ca}^{2+}]$  (33), or in the presence of mutated regulatory proteins unable to completely inhibit acto-myosin interactions in the absence of  $\text{Ca}^{2+}$  (e.g., 20,31). Residual thin-filament activation after  $\text{Ca}^{2+}$  removal that allows the recruitment of new force-generating cross-bridges may be

responsible for the slower relaxation kinetics observed here.

### D137L and D137L/G126R Tms impair the resting properties of myofibrils

As shown in Fig. 2 B, compared with control myofibrils, both D137L and D137L/G126R Tm myofibrils mounted

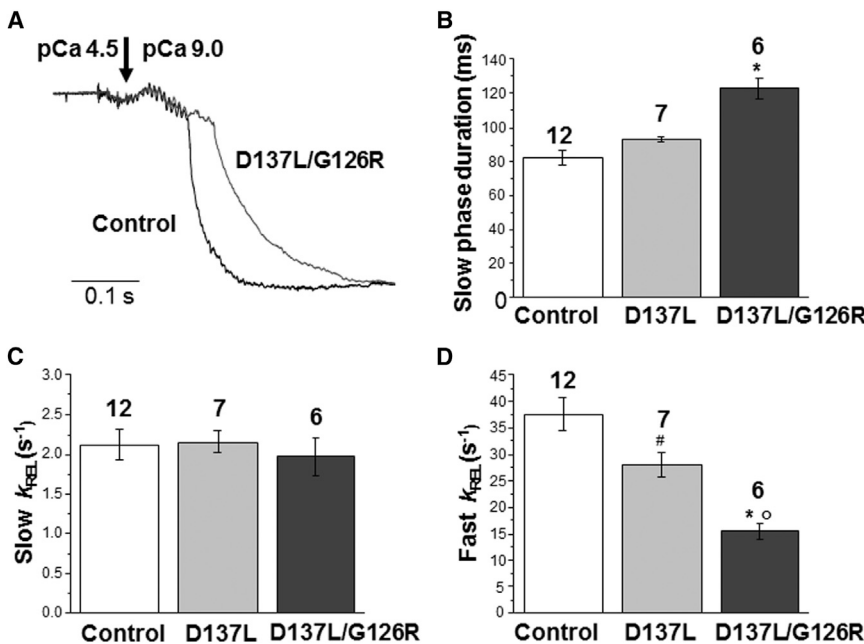


FIGURE 3 Relaxation kinetics of rabbit psoas myofibrils containing recombinant control, D137L, or D137L/G126R  $\alpha\text{Tm}$  at 15°C. (A) Time course of full-force relaxation from maximal activation of representative control and D137L/G126R  $\alpha\text{Tm}$ -reconstituted myofibrils, obtained by fast solution switching from pCa 4.5 back to a pCa 9.0 relaxing solution. The same traces as in Fig. 2 A were normalized and presented on an expanded timescale to show the kinetics of force relaxation. Dark gray trace: control  $\alpha\text{Tm}$  myofibril (duration of slow phase: 129 ms; slow  $k_{\text{REL}}$  = 1.7  $\text{s}^{-1}$ ; fast  $k_{\text{REL}}$  = 13.4  $\text{s}^{-1}$ ). Light gray trace: D137L/G126R  $\alpha\text{Tm}$  myofibril (duration of slow phase: 91 ms; slow  $k_{\text{REL}}$  = 1.6  $\text{s}^{-1}$ ; fast  $k_{\text{REL}}$  = 38.5  $\text{s}^{-1}$ ). (B) Mean values of the duration of slow-phase relaxation. (C) Mean values of the rate of the slow phase of relaxation (slow  $k_{\text{REL}}$ ). (D) Mean values of the rate of the fast phase of relaxation (fast  $k_{\text{REL}}$ ). Histogram columns: control (white), D137L (light gray), and D137L/G126R  $\alpha\text{Tm}$  (dark gray) myofibrils. Bars above the columns are SEM, and the number of myofibrils is shown above the bars. \* $p < 0.0005$  (Student's  $t$ -test) versus the same parameter measured in control  $\alpha\text{Tm}$ -reconstituted myofibrils. # $p < 0.05$  (Student's  $t$ -test) versus the same parameter measured in D137L  $\alpha\text{Tm}$ -reconstituted myofibrils. o $p < 0.002$  (Student's  $t$ -test) versus the same parameter measured in D137L  $\alpha\text{Tm}$ -reconstituted myofibrils.

control  $\alpha\text{Tm}$ -reconstituted myofibrils. # $p < 0.05$  (Student's  $t$ -test) versus the same parameter measured in control  $\alpha\text{Tm}$ -reconstituted myofibrils. o $p < 0.002$  (Student's  $t$ -test) versus the same parameter measured in D137L  $\alpha\text{Tm}$ -reconstituted myofibrils.

on the force-recording apparatus in relaxing solution (see [Materials and Methods](#)) had ~10% shorter initial SLs ( $p < 0.0001$ ) as well as increased resting tension ( $p < 0.01$ ). To understand whether this change was related to the incomplete switch-off state of thin filaments suggested by the alterations of relaxation dynamics, the mean slack SL of control, D137L, and D137L/G126R Tm reconstituted myofibrils was also measured for free myofibrils in relaxing solution, i.e., lying on the bottom of the experimental chamber. In this condition, as shown in [Fig. 4 C](#), the SLs of control  $\alpha\alpha$ Tm myofibrils ( $2.08 \pm 0.02 \mu\text{m}$ ) were significantly longer than those of D137L  $\alpha\alpha$ Tm and D137L/G126R  $\alpha\alpha$ Tm myofibrils, and the difference increased significantly from the single to the double substitution ( $1.95 \pm 0.02 \mu\text{m}$  and  $1.83 \pm 0.03 \mu\text{m}$ , respectively;  $p < 0.0001$ ). This difference was almost completely abolished by the addition of 10 mM BDM, an inhibitor of strong cross-bridge formation ([21,35,39](#)). As shown in [Fig. 4 D](#), BDM did not significantly change the SL of control  $\alpha\alpha$ Tm myofibrils ( $2.13 \pm 0.02 \mu\text{m}$ ), but increased the SLs of both D137L and D137L/G126R  $\alpha\alpha$ Tm myofibrils by ~10–15% ( $2.10 \pm 0.02 \mu\text{m}$  and  $2.07 \pm 0.03 \mu\text{m}$ , respectively), bringing the values close to those measured in control  $\alpha\alpha$ Tm myofibrils. This is a strong indication of the presence of a significant amount of  $\text{Ca}^{2+}$ -independent,

actively cycling cross-bridges in myofibrils replaced with these  $\alpha\alpha$ Tm mutants, and this is greater for the double mutant.

To further investigate the passive properties of D137L and D137L/G126R  $\alpha\alpha$ Tm exchanged myofibrils, quasi-steady-state SL-resting-tension relations were determined under normal relaxing conditions or in the presence of 10 mM BDM ([Fig. 4, A and B](#)). Elongations of increasing extents (up to 30%) were applied to the different myofibril groups, and the SL and resting tension were measured several seconds after each length change (when most of the stress relaxation was over) by imposing large releases that dropped the tension to zero ([Fig. 4 A, inset](#), shows a representative tension trace for a control and a D137L  $\alpha\alpha$ Tm myofibril). The average SL-resting-tension relations in relaxing solution are shown in [Fig. 4 A](#) for control, D137L, and D137L/G126R myofibrils. Clearly, D137L/G126R myofibrils exhibited a higher resting stiffness compared with control myofibrils. In D137L myofibrils, the effect was much smaller and mostly due to the difference in the initial SL. As shown in [Fig. 4 B](#), the addition of 10 mM BDM almost completely abolished these differences, further supporting the hypothesis that these mutants prevent full inhibition of the acto-myosin interaction at low resting  $[\text{Ca}^{2+}]$ .

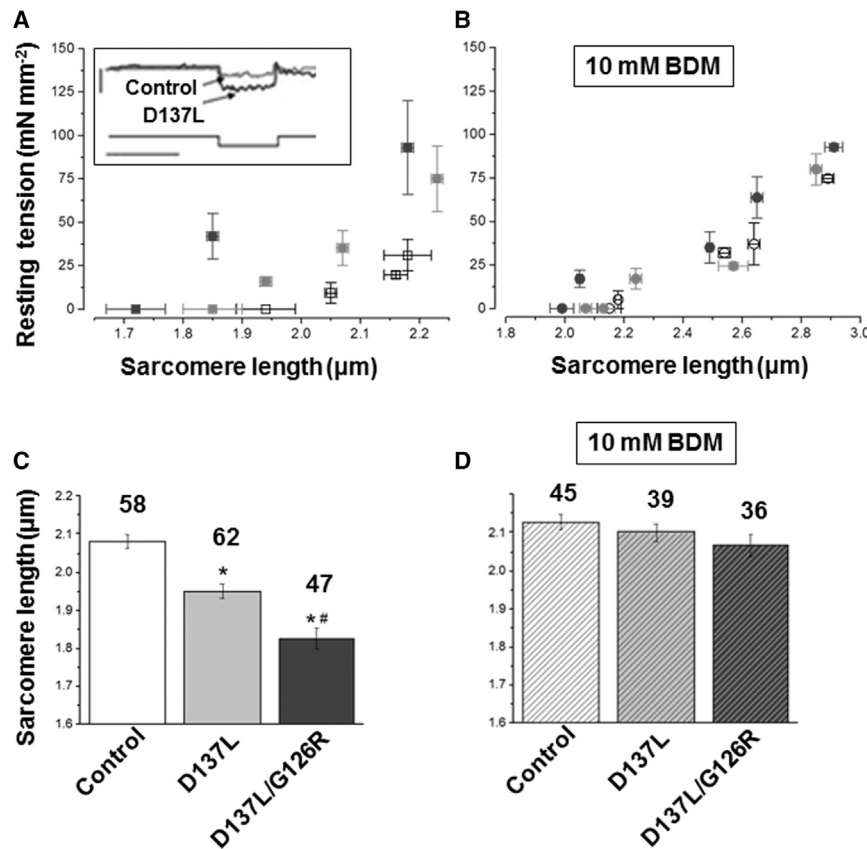


**FIGURE 4** SL and  $\text{Ca}^{2+}$ -independent tension of control, D137L, and D137L/G126R  $\alpha\alpha$ Tm-reconstituted myofibrils. (A) Average SL-resting-tension relationships of myofibrils extracted and reconstituted with control (white square), D137L (light gray square), or D137L/G126R (dark gray square)  $\alpha\alpha$ Tm. Data points at different SLs are means  $\pm$  SEM (vertical and horizontal bars) of resting-tension values measured in five to nine individual myofibrils. Inset, lower trace: representative trace of 30%  $I_0$  step release applied to a myofibril at pCa 9.0; upper traces:  $\text{Ca}^{2+}$ -independent force response for control  $\alpha\alpha$ Tm and D137L  $\alpha\alpha$ Tm mounted myofibrils. Tension calibration (vertical bar): 40 mN  $\text{mm}^{-2}$ ; time calibration (horizontal bar): 50 ms. (B) Effect of 10 mM BDM on average SL-resting-tension relationships for the different groups of Tm-Tn-replaced myofibrils. (C) Mean slack SL of free control, D137L, and D137L/G126R Tm-reconstituted myofibrils measured in relaxing solution. The SLs in the presence of mutant  $\alpha\alpha$ Tm are significantly shorter compared with control  $\alpha\alpha$ Tm myofibrils ( $*p < 0.0001$ ). SLs are also considerably shorter in D137L/G126R  $\alpha\alpha$ Tm myofibrils than in D137L  $\alpha\alpha$ Tm myofibrils ( $\#p < 0.01$ ). (D) Effect of 10 mM BDM on the mean slack SLs of control, D137L, and D137L/G126R  $\alpha\alpha$ Tm-reconstituted myofibrils. All values ( $\mu\text{m}$ ) are given as mean  $\pm$  SEM: control  $\alpha\alpha$ Tm  $2.08 \pm 0.02$ , control + BDM  $2.13 \pm 0.02$ ; D137L  $\alpha\alpha$ Tm  $1.95 \pm 0.02$ , D137L + BDM  $2.10 \pm 0.02$ ; D137L/G126R  $\alpha\alpha$ Tm  $1.83 \pm 0.03$ , D137L/G126R + BDM  $2.07 \pm 0.03$ . The number of myofibrils is given above the bars.

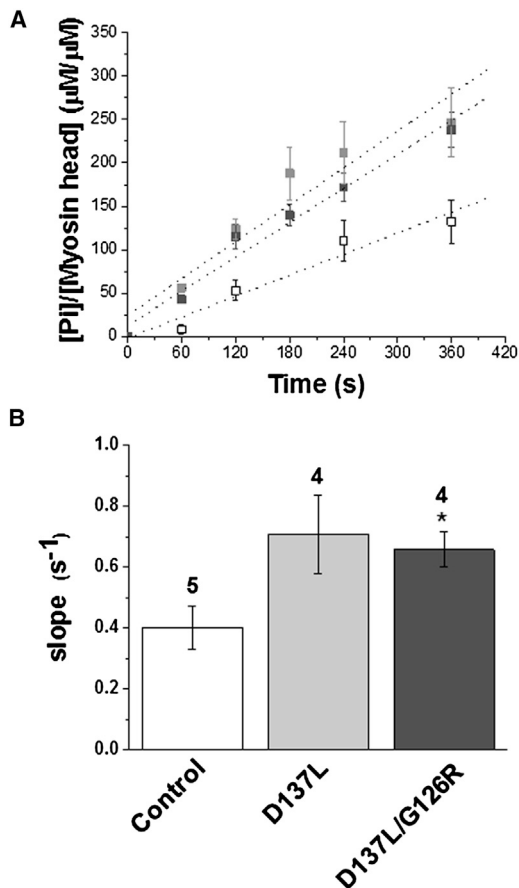


FIGURE 5 Myofibrillar ATPase at low  $[Ca^{2+}]$  is much greater for reconstituted myofibrils containing D137L (light gray square) and D137L/G126R (dark gray square) compared with control  $\alpha\alpha$ Tm (white square) (30°C). (A) ATPase activity of reconstituted myofibrils measured in relaxing solution (pCa 9.0). Each point is the mean  $\pm$  SEM of four measurements (five for control  $\alpha\alpha$ Tm). The steady-state ATPase rate was obtained from regression lines (dotted lines) fitted on all individual data points. (B) Average slope of regression lines (steady-state rate;  $s^{-1}$ ) of replaced myofibrils: control  $\alpha\alpha$ Tm  $0.40 \pm 0.07$ ; D137L  $\alpha\alpha$ Tm  $0.71 \pm 0.13$ ; D137L/G126R  $\alpha\alpha$ Tm  $0.66 \pm 0.06$ . The steady-state rate was significantly increased in D137L/G126R  $\alpha\alpha$ Tm compared with control  $\alpha\alpha$ Tm myofibrils ( $*p < 0.05$ , Student's *t*-test).

### D137L and D137L/G126R Tms increase the resting ATPase activity of myofibrils

We further investigated the greater degree of  $Ca^{2+}$ -independent active cross-bridge formation in D137L and D137L/G126R  $\alpha\alpha$ Tm compared with control myofibrils by measuring steady-state ATPase activity in relaxing solution (see Materials and Methods). Fig. 5 A shows mean data points from four to five experiments measuring the time course of inorganic phosphate ( $P_i$ ) formation after addition of a large excess of Mg-ATP to myofibril batches collected at different times after trichloroacetic acid quench (60–360 s). The initial rapid transient formation of  $P_i$  was not resolved in our conditions. As shown in Fig. 5 A, myofibrils reconstituted with  $\alpha\alpha$ Tm with single or double stabilizing substitutions showed

a clear increase in resting steady-state ATP hydrolysis when compared with control  $\alpha\alpha$ Tm reconstituted myofibrils. The increase was significant for D137L/G126R  $\alpha\alpha$ Tm myofibrils ( $p < 0.05$ ). For D137L  $\alpha\alpha$ Tm-enriched myofibrils, the effect was somewhat smaller ( $p = 0.06$ ). The mean slope values of the regression lines used to estimate the steady-state ATP hydrolysis rate were  $0.40 \pm 0.07 s^{-1}$ ,  $0.71 \pm 0.13 s^{-1}$ , and  $0.66 \pm 0.06 s^{-1}$  for control, D137L, and D137L/G126R  $\alpha\alpha$ Tm, respectively (Fig. 5 B). These results further strengthen the hypothesis regarding an inhibition of the switch-off mechanism associated with the presence of D137L or D137L/G126R  $\alpha\alpha$ Tm in the thin filament.

### D137L and D137L/G126R Tms increase the apparent $Ca^{2+}$ sensitivity of tension

We also investigated the  $Ca^{2+}$  dependence of tension generation in D137L  $\alpha\alpha$ Tm-replaced myofibrils by comparing force generation at submaximal and maximal  $[Ca^{2+}]$  activations. Control and D137L  $\alpha\alpha$ Tm myofibrils were activated by rapid solution switching, first submaximally (pCa 5.95) and then maximally (pCa 4.50). Representative tracings of these  $Ca^{2+}$ -jump experiments are shown in Fig. 6 A together with the mean tension ratio values (Fig. 6 B). The ratio of submaximal to maximal tension was significantly higher (~50%) in D137L  $\alpha\alpha$ Tm compared with control  $\alpha\alpha$ Tm-replaced myofibrils ( $p < 0.02$ ). These results apparently indicate that D137L  $\alpha\alpha$ Tm imparts a significant increase of myofilament  $Ca^{2+}$  sensitivity. However, this could also be explained by the observation of the involvement of active cross-bridges in the absence of  $Ca^{2+}$ , whose contribution decreases with increasing  $Ca^{2+}$  concentration. This would produce a force/pCa<sup>2+</sup> curve shifted to lower  $[Ca^{2+}]$  (20) without an actual change in  $Ca^{2+}$  sensitivity.

### C-terminal truncated cTnI shows inhibition of relaxation similar to that observed for D137L and D137L/G126R Tms in myofibrils

Functional modifications similar to those reported here for D137L and D137L/G126R substitutions in  $\alpha\alpha$ Tm were also observed in rabbit psoas myofibrils exchanged with a truncated TnI subunit (cTnI<sub>1-192</sub>) that was unable to fully inhibit acto-myosin interactions in the absence of  $Ca^{2+}$  (24,31). As shown in Fig. 7 A, when a C-terminal truncated form of TnI (cTnI<sub>1-192</sub>) was replaced in myofibrils for full-length TnI, full-force relaxation from maximal activation was slowed down compared with controls, i.e., compared with unexchanged myofibrils (native (Nat)) or with myofibrils replaced by full-length cTnI (cTnI<sub>FL</sub>). This is similar to what was observed for D137L and D137L/G126R  $\alpha\alpha$ Tm mutations, i.e., a significant increase in the duration of the slow phase of relaxation (Fig. 7 B) and a decrease in both rates of relaxation (Fig. 7, C and D), which was significant for the fast phase ( $*p < 0.01$ ). Moreover, the

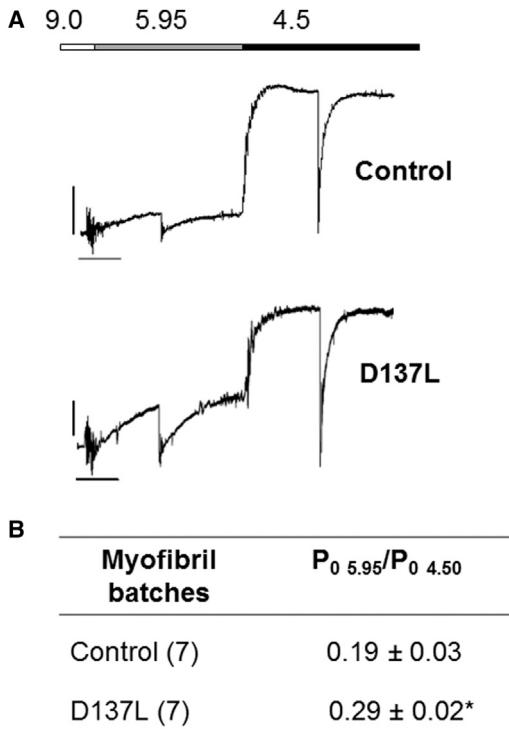


FIGURE 6 D137L  $\alpha\alpha$ Tm-reconstituted myofibrils show a greater active tension than control at submaximal  $\text{Ca}^{2+}$  activation. (A) Myofibrils replaced with control  $\alpha\alpha$ Tm (upper trace) and D137L  $\alpha\alpha$ Tm (lower trace) were activated at pCa 5.95 and then subjected to  $[\text{Ca}^{2+}]$  jumps to pCa 4.50 at  $15^\circ\text{C}$ . At each level of  $\text{Ca}^{2+}$  activation, a release-restretch was applied to the preparation under steady-state conditions of tension generation. Bars above the traces correspond to the timing of the solution change, and numbers correspond to the pCa values of relaxing, submaximal, and maximal activating solutions. Tension calibration (vertical bar):  $100\ \text{mN mm}^{-2}$ ; time calibration (horizontal bar): 1 s. Control  $\alpha\alpha$ Tm myofibril: SL  $2.31\ \mu\text{m}$ , resting tension  $20\ \text{mN mm}^{-2}$ ,  $P_{0\ 5.95}/P_{0\ 4.50} = 0.17$ ; D137L  $\alpha\alpha$ Tm myofibril: SL  $2.18\ \mu\text{m}$ , resting tension  $90\ \text{mN mm}^{-2}$ ,  $P_{0\ 5.95}/P_{0\ 4.50} = 0.36$ . (B) Mean values for the ratio of submaximal pCa 5.95 to maximal pCa 4.50 activated tension obtained from  $[\text{Ca}^{2+}]$  jump experiments in control and D137L  $\alpha\alpha$ Tm-replaced myofibrils. Values are given as means  $\pm$  SEM; numbers in parentheses are the number of myofibrils;  $*p < 0.02$ , Student's *t*-test.

BDM-sensitive increase in resting tension (Fig. 7 E) observed in the presence of cTnI<sub>1-192</sub> is almost superimposable with that observed for D137L and D137L/G126R  $\alpha\alpha$ Tm mutations. Because structural (2) and photo-cross-linking (22) studies have shown that the C-terminal region of TnI interacts with actin and the central region of  $\alpha\alpha$ Tm (at residue 146) in a  $\text{Ca}^{2+}$ -dependent manner, the removal of that region would critically reduce inhibition of actomyosin interactions in the absence of  $\text{Ca}^{2+}$  (40). A loss of interaction of C-terminal TnI with the region of  $\alpha\alpha$ Tm around 146 due to the 137 and 126 mutations could explain the inhibition of relaxation observed here (see Discussion).

## DISCUSSION

In this study, we used tension measurements on single myofibrils (28–30) to study the functional impact of

substituting stabilizing canonical amino acid residues for highly conserved native residues in  $\alpha\alpha$ Tm at positions 137 and both 137 and 126 (D137L and D137L/G126R, respectively). All of the Tm forms used in this study had the C190A substitution, eliminating the possibility of sulfhydryl oxidation and thereby mimicking the physiological reduced state of Tm in sarcomeres of rabbit psoas muscle (41). Only minor structural changes occur when Cys190 is replaced by an Ala (11,12), and myofibrils reconstituted with C190A Tm-Tn (controls) show no functional alteration compared with myofibrils reconstituted with native Tm (data not shown). C190A Tm-Tn-replaced myofibrils were then used as a control for a comparative study with D137L or D137L/G126R Tm-Tn to eliminate the possibility of a change in the properties of myofibrils subjected to the Tm-Tn extraction-reconstitution procedure (18,27). Moreover, Tm in these native myofibrils consists of a 3:1 to 4:1 mixture of  $\alpha$  and  $\beta$  isoforms with a 50:50 mixture of  $\alpha\alpha$ Tm and  $\alpha\beta$ Tm (42). By replacing  $\alpha\beta$ Tm with  $\alpha\alpha$ Tm, we minimized the possible influence of  $\alpha\beta$ Tm on  $\text{Ca}^{2+}$  regulation (19).

## Relaxation impairment and the three-state theory

In contrast to the lack of appreciable effect on the kinetics of activation and active force at saturating  $\text{Ca}^{2+}$ , the presence of Tm mutants importantly affected myofibril relaxation with the following functional consequences: a prolongation of relaxation (Fig. 3), a decrease in initial SL eliminated by BDM (Fig. 4), a twofold increase in resting tension (Fig. 2 B), a 50% increase in resting ATPase (Fig. 5), and an apparent increase in  $\text{Ca}^{2+}$  sensitivity (Fig. 6). Relaxation from the fully turned on myofibril system by  $\text{Ca}^{2+}$  removal consisted of two kinetic processes: a slow linear tension decrease and a fast exponential tension decrease (Fig. 3 A). The former reflects cross-bridge detachment from maximal  $\text{Ca}^{2+}$  under isometric conditions of the sarcomeres. The latter is initiated by sarcomere give and dominated by sarcomere dynamics (43,44), and its rate mainly depends on the isoform of the myosin heavy-chain motor (34). The persistence of cycling cross-bridges after  $\text{Ca}^{2+}$  removal can keep the system active, resulting in a prolongation of the duration of the slow phase and a slowing down of the fast relaxation phase (see Fig. 5 C in Ref. 33). These results point toward the involvement of force-generating cross-bridges in inhibiting relaxation, and can be explained by shifting equilibria among the three states of muscle regulation (blocked-closed-open), which relates the properties of myosin binding to actin-TmTn (45) with the Tm structural position on actin (3,4). In the three-state model, Tm bound to actin equilibrates among the blocked-closed-open states, with  $\text{Ca}^{2+}$  allosterically affecting the first equilibrium and myosin the second equilibrium. The open state is the active state and is often termed the M-induced or M state.



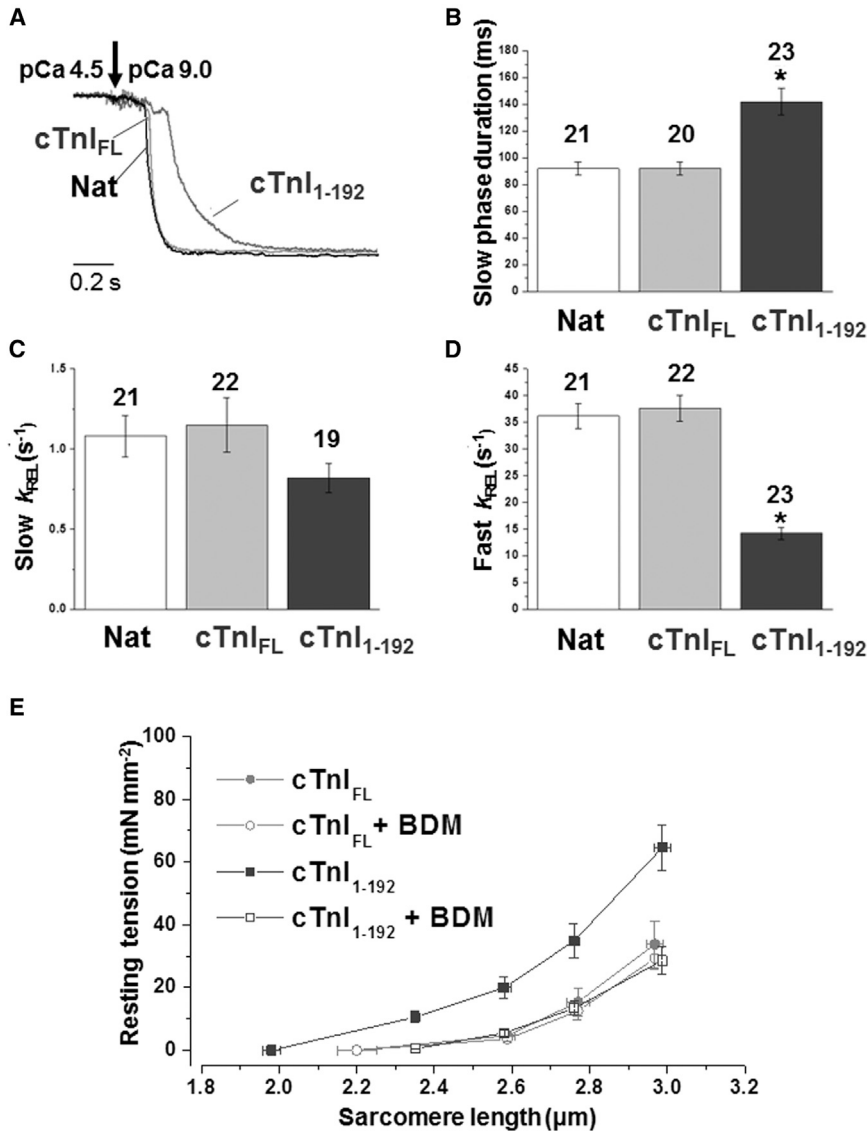


FIGURE 7 Relaxation kinetics and SL-resting-tension relationship of rabbit psoas myofibrils after exchange of endogenous TnI with a C-terminal truncated TnI form (cTnI<sub>1-192</sub>) at 15°C. (A) Time course of full-force relaxation from maximal activation of native (unexchanged) myofibrils (Nat, black line) and myofibrils in which whole native Tn had been replaced (by exchange) by cTn, including either the full-length (cTnI<sub>FL</sub>, gray line) or truncated (1–192 (cTnI<sub>1-192</sub>), dark gray line) cTnI subunit, normalized and presented on an expanded timescale to show the kinetics of force relaxation. (B) Mean values of the duration of slow-phase relaxation. (C) Mean values of the rate of the slow phase of relaxation (slow  $k_{REL}$ ). (D) Mean values of the rate of the fast phase of relaxation (fast  $k_{REL}$ ). \* $p < 0.01$  versus the same parameter measured in cTnI<sub>FL</sub> and native unexchanged myofibrils. The number of myofibrils is given above the bars. (E) Average SL-resting-tension relationships of myofibrils replaced with either cTnI<sub>FL</sub> (gray solid circle) or cTnI<sub>1-192</sub> (dark gray square). BDM (10 mM) completely abolishes the difference in passive tension (open square, cTnI<sub>1-192</sub>; open circle, cTnI<sub>FL</sub>). Vertical and horizontal bars are SEM. Resting tension and mean SL were measured under quasi-steady-state conditions.

The observation that the system is still active in the absence of  $Ca^{2+}$  shows that there is a contribution from the open- or myosin-induced state that could be caused by a loss of blocked state, leading to increased myosin binding in the closed state or a direct effect of strong myosin binding to increase the open state. We recently proposed a myosin-induced open state to explain relaxation effects due to mutations that cause hypertrophic cardiomyopathy (HCM), termed  $M^-$  (20). The  $M^-$ -open state is free of  $Ca^{2+}$ , in contrast to the  $M^+$ -open state, which has  $Ca^{2+}$  bound to TnC. In the open state, whether  $Ca^{2+}$  is present ( $M^+$ ) or not ( $M^-$ ), Tm does not block myosin binding and therefore allows active cycling. The increase of the duration of the slow phase of relaxation, the slowing of the fast phase (Fig. 3), and the increase of the residual resting tension for the mutants (Fig. 2 B) indicate a greater contribution of the  $M^-$  state in the case of the mutants. The

apparent increase in the  $Ca^{2+}$  sensitivity of tension (Fig. 6), however, is due to the contribution of the residual tension produced by the  $M^-$  state, which decreases as the  $[Ca^{2+}]$  increases (20).

### D137L and D137L/G126R Tm interactions in the thin filament

In view of the coupled equilibria in the three-state theory, a changed interaction between Tm and any of the other components (actin, Tn, and myosin) could explain the inability of muscle to completely relax in the absence of  $Ca^{2+}$ . The inhibition of relaxation observed for these mutants may be explained by our observation that cTnI containing a C-terminal truncation, cTnI<sub>1-192</sub>, produced relaxation properties very similar to those found for the Tm mutants, e.g., a slowing down and incomplete inhibition of tension (Fig. 7). This

effect is not due to the presence in skeletal thin filaments of the cardiac isoform of TnI (presenting an N-terminal extension), as proved by the lack of effects in cTnI-replaced myofibrils compared with native control samples. Structural studies with cTnI<sub>1-192</sub> have indicated that the C-terminal region does affect the position or state of Tm on actin (39). At the same time, functional studies have indicated that when cTnI<sub>1-192</sub> is present in the Tn complex, cross-bridge formation in the absence of Ca<sup>2+</sup> is not fully inhibited, with impaired inhibition of the resting ATPase of reconstituted cardiac systems (46), impaired relaxation, and an apparent increase in the Ca<sup>2+</sup> sensitivity of replaced cardiac myofibrils (31). Similar effects were produced with the TnI HCM mutant R146W-cTnI (47), which appeared to shift the equilibrium away from the blocked state (20). Interestingly, cross-linking (22) and structural (48) data show an interaction of TnI with Tm in the absence of Ca<sup>2+</sup>. Thus, loss of this interaction with the Tm mutants appears to be the cause of the relaxation impairment. Our previous studies showed that these mutations increase the stability or dynamic rigidity of Tm in solution (9,10,12). It is possible that this loss of conformational mobility contributes to the loss of a specific interaction between Tm and a region in the C-terminus of TnI.

Previous results have shown that these stabilizing mutants do not alter the Tm-actin binding capability (9,16), likely preserving the preshaped Tm configuration (Gestalt-binding (49)) despite the presence of some long-range overall molecular straightening and local stiffening (11). Myosin has been shown to dissociate TnI from actin<sub>7</sub>TmTnI (22), indicating a direct shift in the actin-Tm state from blocked to open. Also, evidence has been obtained for an interaction between myosin and Tm in the M state from cross-linking studies (50) and structural studies (51), which may be facilitated by these mutants. Evidence for changed myosin-Tm interactions and TnI-Tm interactions could be obtained from binding studies of myosin subfragment 1 and TnI with mutant Tm in thin filaments.

In view of the increased duration of the slow relaxation phase in the myofibril, another connection to the increased stability/rigidity properties of the mutants is possible. Tm in the thin filament interacts with seven actin subunits and with itself end-to-end, forming a continuous strand along actin. The cooperative unit size,  $n$ , in the reconstituted thin filament (actin<sub>7</sub>TmTn), however, was shown to be  $n = 10-12$ , due to strong end-to-end interactions facilitated by Tn (20). The greater duration of the slow phase of relaxation for the mutants observed here suggests a greater communication between neighboring structural units, with a bound head at one actin site keeping many neighboring sites open via a more rigid Tm. For these mutants, it would be interesting to verify this proposed mechanism for the change in  $n$  by conducting in vitro kinetic studies on reconstituted thin filaments with labeled Tm, as previously performed on native systems (20).

## HCM mutants E180G and D175N and impairment of relaxation

The contribution of the M<sup>-</sup>-active state has been proposed to explain similar impaired relaxation properties of thin-filament proteins containing mutations that cause HCM (4,20). In particular,  $\alpha$ Tm E180G and D175N have shown a similar incomplete relaxation and apparent increase in Ca<sup>2+</sup> sensitivity (52-54). In these cases, the effects were also explained by a shift in the equilibrium from the blocked state to the closed state, resulting in increased myosin binding to produce the M<sup>-</sup>-open state. In contrast to the mutant Tms examined here, in which increased rigidity was observed, the inhibition of relaxation observed for the HCM mutants was associated with decreased rigidity or increased flexibility, possibly affecting the Tm-actin interaction. Other HCM mutations in muscle proteins can produce inhibition of relaxation depending upon the effect on the coupled equilibria (blocked-closed-open) in this multicomponent allosteric system (20).

## Discrepancies with previous studies

The results of this investigation do not fully agree with those reported in a previous study involving a transgenic (TG) mouse model for D137L  $\alpha$ Tm (17). In that study, an in vitro characterization of D137L  $\alpha$ Tm confirmed previous data (9) as well as a long-range molecular rearrangement seen in structural studies (11,12). However, the TG mouse study (17) reported that D137L  $\alpha$ Tm had no effect on acto-myosin ATPase of reconstituted myofilaments, whereas a clear increase had been previously reported (9) and is confirmed by our data. Moreover, the D137L TG mouse showed a clear decrease of in situ cardiac function and cardiomyocyte contractility in terms of force and Ca<sup>2+</sup> sensitivity, which does not agree with our observations in Tm-Tn-replaced rabbit psoas myofibrils. This discrepancy could be explained by the different experimental conditions used (cardiac versus skeletal) as well as the uncertain assessment of protein content (isoforms and posttranslational modified forms) in the sarcomeres of the TG mice. Studies of the functional consequences of replacing D137L or D137L/G126R  $\alpha$ Tm in cardiac myofibrils could help to clarify this point.

## CONCLUSIONS

We used the novel, to our knowledge, approach of monitoring the mechanical properties of single myofibrils containing mutant Tms with one or two stabilizing amino acids substituted for native ones, and found that regulatory function was compromised. The myofibrils relaxed more slowly and incompletely, indicating an increased contribution of the open state in the absence of Ca<sup>2+</sup> (M<sup>-</sup>). These studies emphasize that the amino acid sequence of Tm did

not evolve for maximum stability, but rather reflects the properties that Tm needs to function within the finely coupled equilibria of muscle regulation involving interactions with actin, Tn, and myosin. Its sequence reflects the need for Tm to 1) be water soluble and properly folded under physiological conditions; 2) interact sufficiently weakly with actin to allow Tm movement upon  $\text{Ca}^{2+}$  binding to Tn; 3) interact with Tn and actin strongly enough to block initial weak myosin binding, yet allow force-generating, strong myosin binding; 4) interact end-to-end with itself to provide continuity; and 5) have the right flexibility to facilitate conformational changes during changing protein interactions and to be able to transmit perturbing signals produced by Tn and myosin. This study also provides a basis for understanding how single Tm mutations involved in cardiomyopathies can compromise function.

## AUTHOR CONTRIBUTIONS

S.S.L., D.I.L., C.P., and C.T. designed the research. N.P. and B.S. performed the research. A.M.M. and D.I.L. prepared the proteins. B.S., C.P., S.S.L., D.I.L., and C.T. analyzed and interpreted the data, and wrote the manuscript. All authors edited the manuscript.

## ACKNOWLEDGMENTS

The authors thank Sig. Alessandro Aiazzi for skillful technical advice and design, Dr. John Sumida for early D137L characterization, Prof. Michael Geeves (sTn) and Prof. Ger Stienen (cTnI<sub>1-192</sub> and cTnI<sub>FL</sub>) for the generous gifts of proteins, and Prof. M. Geeves and Dr. Andrey Tsaturyan for helpful discussions.

This work was supported by the 7th Framework Program of the European Union (STREP Project BIG-HEART, grant agreement 241577), Telethon-Italy (GGP07133), the Ministero Italiano dell'Università e Ricerca Scientifica MIUR (PRIN 2010R8JK2X\_002 to B.S., N.P., C.P., and C.T.), and the Russian Science Foundation (grant 16-14-10199 to A.M.M. and D.I.L.).

## REFERENCES

- Gordon, A. M., E. Homsher, and M. Regnier. 2000. Regulation of contraction in striated muscle. *Physiol. Rev.* 80:853–924.
- Galińska-Rakoczy, A., P. Engel, ..., W. Lehman. 2008. Structural basis for the regulation of muscle contraction by troponin and tropomyosin. *J. Mol. Biol.* 379:929–935.
- Lehman, W. 2016. Thin filament structure and the steric blocking model. *Compr. Physiol.* 6:1043–1069.
- Geeves, M. A. 2012. Thin filament regulation. *Compr. Biophys.* 4:251–267.
- Moore, J. R., S. G. Campbell, and W. Lehman. 2016. Structural determinants of muscle thin filament cooperativity. *Arch. Biochem. Biophys.* 594:8–17.
- Perry, S. V. 2001. Vertebrate tropomyosin: distribution, properties and function. *J. Muscle Res. Cell Motil.* 22:5–49.
- Nevzorov, I. A., and D. I. Levitsky. 2011. Tropomyosin: double helix from the protein world. *Biochemistry (Mosc.)* 76:1507–1527.
- Robinson, P., P. J. Griffiths, ..., C. S. Redwood. 2007. Dilated and hypertrophic cardiomyopathy mutations in troponin and alpha-tropomyosin have opposing effects on the calcium affinity of cardiac thin filaments. *Circ. Res.* 101:1266–1273.
- Sumida, J. P., E. Wu, and S. S. Lehrer. 2008. Conserved Asp-137 imparts flexibility to tropomyosin and affects function. *J. Biol. Chem.* 283:6728–6734.
- Nevzorov, I. A., O. P. Nikolaeva, ..., D. I. Levitsky. 2011. Conserved noncanonical residue Gly-126 confers instability to the middle part of the tropomyosin molecule. *J. Biol. Chem.* 286:15766–15772.
- Moore, J. R., X. Li, ..., W. Lehman. 2011. Structural implications of conserved aspartate residues located in tropomyosin's coiled-coil core. *BioArchitecture*. 1:250–255.
- Matyushenko, A. M., N. V. Artemova, ..., D. I. Levitsky. 2015. Effects of two stabilizing substitutions, D137L and G126R, in the middle part of  $\alpha$ -tropomyosin on the domain structure of its molecule. *Biophys. Chem.* 196:77–85.
- Zheng, W., S. E. Hitchcock-DeGregori, and B. Barua. 2016. Investigating the effects of tropomyosin mutations on its flexibility and interactions with filamentous actin using molecular dynamics simulation. *J. Muscle Res. Cell Motil.* 37:131–147.
- Nabiev, S. R., D. A. Ovsyannikov, ..., S. Y. Bershitsky. 2015. Stabilizing the central part of tropomyosin increases the bending stiffness of the thin filament. *Biophys. J.* 109:373–379.
- Shchepkin, D. V., A. M. Matyushenko, ..., D. I. Levitsky. 2013. Stabilization of the central part of tropomyosin molecule alters the  $\text{Ca}^{2+}$ -sensitivity of actin-myosin interaction. *Acta Naturae*. 5:126–129.
- Matyushenko, A. M., N. V. Artemova, ..., D. I. Levitsky. 2014. Structural and functional effects of two stabilizing substitutions, D137L and G126R, in the middle part of  $\alpha$ -tropomyosin molecule. *FEBS J.* 281:2004–2016.
- Yar, S., S. A. Chowdhury, ..., R. J. Solaro. 2013. Conserved Asp-137 is important for both structure and regulatory functions of cardiac  $\alpha$ -tropomyosin ( $\alpha$ -TM) in a novel transgenic mouse model expressing  $\alpha$ -TM-D137L. *J. Biol. Chem.* 288:16235–16246.
- Scellini, B., N. Piroddi, ..., C. Tesi. 2010. Extraction and replacement of the tropomyosin-troponin complex in isolated myofibrils. *Adv. Exp. Med. Biol.* 682:163–174.
- Scellini, B., N. Piroddi, ..., C. Tesi. 2015. Impact of tropomyosin isoform composition on fast skeletal muscle thin filament regulation and force development. *J. Muscle Res. Cell Motil.* 36:11–23.
- Lehrer, S. S., and M. A. Geeves. 2014. The myosin-activated thin filament regulatory state,  $\text{M}^-$ -open: a link to hypertrophic cardiomyopathy (HCM). *J. Muscle Res. Cell Motil.* 35:153–160.
- McKillop, D. F., N. S. Fortune, ..., M. A. Geeves. 1994. The influence of 2,3-butanedione 2-monoxime (BDM) on the interaction between actin and myosin in solution and in skinned muscle fibres. *J. Muscle Res. Cell Motil.* 15:309–318.
- Mudalige, W. A., T. C. Tao, and S. S. Lehrer. 2009.  $\text{Ca}^{2+}$ -dependent photocrosslinking of tropomyosin residue 146 to residues 157–163 in the C-terminal domain of troponin I in reconstituted skeletal muscle thin filaments. *J. Mol. Biol.* 389:575–583.
- Scellini, B., C. Ferrara, ..., C. Tesi. 2012. Tropomyosin D137L/C190A of reduced flexibility increases submaximal  $\text{Ca}^{2+}$ -activated tension in skeletal muscle myofibrils after troponin-tropomyosin removal and reconstitution. *Biophys. J.* 102:230–231a.
- Belus, A., N. A. Narolska, ..., C. Poggesi. 2007. Human C-terminal truncated cardiac troponin I exchanged into rabbit psoas myofibrils is unable to fully inhibit actin-myosin interaction in the absence of  $\text{Ca}^{2+}$ . *Biophys. J.* 92:629a.
- Geeves, M. A., S. E. Hitchcock-DeGregori, and P. W. Gunning. 2015. A systematic nomenclature for mammalian tropomyosin isoforms. *J. Muscle Res. Cell Motil.* 36:147–153.
- Monteiro, P. B., R. C. Lataro, ..., F. C. Reinach. 1994. Functional alpha-tropomyosin produced in *Escherichia coli*. A dipeptide extension can substitute the amino-terminal acetyl group. *J. Biol. Chem.* 269:10461–10466.
- Siththanandan, V. B., L. S. Tobacman, ..., E. Homsher. 2009. Mechanical and kinetic effects of shortened tropomyosin reconstituted into myofibrils. *Pflugers Arch.* 458:761–776.

28. Colomo, F., N. Piroddi, ..., C. Tesi. 1997. Active and passive forces of isolated myofibrils from cardiac and fast skeletal muscle of the frog. *J. Physiol.* 500:535–548.
29. Colomo, F., S. Nencini, ..., C. Tesi. 1998. Calcium dependence of the apparent rate of force generation in single striated muscle myofibrils activated by rapid solution changes. *Adv. Exp. Med. Biol.* 453:373–381, discussion 381–382.
30. Tesi, C., F. Colomo, ..., C. Poggesi. 2000. The effect of inorganic phosphate on force generation in single myofibrils from rabbit skeletal muscle. *Biophys. J.* 78:3081–3092.
31. Narolska, N. A., N. Piroddi, ..., G. J. Stienen. 2006. Impaired diastolic function after exchange of endogenous troponin I with C-terminal truncated troponin I in human cardiac muscle. *Circ. Res.* 99:1012–1020.
32. Brenner, B. 1988. Effect of  $\text{Ca}^{2+}$  on cross-bridge turnover kinetics in skinned single rabbit psoas fibers: implications for regulation of muscle contraction. *Proc. Natl. Acad. Sci. USA.* 85:3265–3269.
33. Tesi, C., N. Piroddi, ..., C. Poggesi. 2002. Relaxation kinetics following sudden  $\text{Ca}^{2+}$  reduction in single myofibrils from skeletal muscle. *Biophys. J.* 83:2142–2151.
34. Poggesi, C., C. Tesi, and R. Stehle. 2005. Sarcomeric determinants of striated muscle relaxation kinetics. *Pflugers Arch.* 449:505–517.
35. Tesi, C., F. Colomo, ..., C. Poggesi. 2002. Characterization of the cross-bridge force-generating step using inorganic phosphate and BDM in myofibrils from rabbit skeletal muscles. *J. Physiol.* 541:187–199.
36. Herrmann, C., C. Lionne, ..., T. Barman. 1994. Correlation of ActoS1, myofibrillar, and muscle fiber ATPases. *Biochemistry.* 33:4148–4154.
37. Ohno, T., and T. Kodama. 1991. Kinetics of adenosine triphosphate hydrolysis by shortening myofibrils from rabbit psoas muscle. *J. Physiol.* 441:685–702.
38. Nixon, B. R., B. Liu, ..., B. J. Biesiadecki. 2013. Tropomyosin Ser-283 pseudo-phosphorylation slows myofibril relaxation. *Arch. Biochem. Biophys.* 535:30–38.
39. Galińska, A., V. Hatch, ..., D. B. Foster. 2010. The C terminus of cardiac troponin I stabilizes the  $\text{Ca}^{2+}$ -activated state of tropomyosin on actin filaments. *Circ. Res.* 106:705–711.
40. Regnier, M., C. Morris, and E. Homsher. 1995. Regulation of the cross-bridge transition from a weakly to strongly bound state in skinned rabbit muscle fibers. *Am. J. Physiol.* 269:C1532–C1539.
41. Lehrer, S. S., S. Ly, and F. Fuchs. 2011. Tropomyosin is in a reduced state in rabbit psoas muscle. *J. Muscle Res. Cell Motil.* 32:19–21.
42. Lehrer, S. S. 1975. Intramolecular crosslinking of tropomyosin via disulfide bond formation: evidence for chain register. *Proc. Natl. Acad. Sci. USA.* 72:3377–3381.
43. Stehle, R., M. Krüger, and G. Pfitzer. 2002. Force kinetics and individual sarcomere dynamics in cardiac myofibrils after rapid  $\text{Ca}^{2+}$  changes. *Biophys. J.* 83:2152–2161.
44. Brunello, E., L. Fusi, ..., M. Irving. 2009. Structural changes in myosin motors and filaments during relaxation of skeletal muscle. *J. Physiol.* 587:4509–4521.
45. McKillop, D. F., and M. A. Geeves. 1993. Regulation of the interaction between actin and myosin subfragment 1: evidence for three states of the thin filament. *Biophys. J.* 65:693–701.
46. Foster, D. B., T. Noguchi, ..., J. E. Van Eyk. 2003. C-terminal truncation of cardiac troponin I causes divergent effects on ATPase and force: implications for the pathophysiology of myocardial stunning. *Circ. Res.* 93:917–924.
47. Kobayashi, T., and R. J. Solaro. 2006. Increased  $\text{Ca}^{2+}$  affinity of cardiac thin filaments reconstituted with cardiomyopathy-related mutant cardiac troponin I. *J. Biol. Chem.* 281:13471–13477.
48. Yang, S., L. Barbu-Tudoran, ..., W. Lehman. 2014. Three-dimensional organization of troponin on cardiac muscle thin filaments in the relaxed state. *Biophys. J.* 106:855–864.
49. Holmes, K. C., and W. Lehman. 2008. Gestalt-binding of tropomyosin to actin filaments. *J. Muscle Res. Cell Motil.* 29:213–219.
50. Golitsina, N. L., and S. S. Lehrer. 1999. Smooth muscle alpha-tropomyosin crosslinks to caldesmon, to actin and to myosin subfragment 1 on the muscle thin filament. *FEBS Lett.* 463:146–150.
51. von der Ecken, J., M. Müller, ..., S. Raunser. 2015. Structure of the F-actin-tropomyosin complex. *Nature.* 519:114–117.
52. Bai, F., L. Wang, and M. Kawai. 2013. A study of tropomyosin's role in cardiac function and disease using thin-filament reconstituted myocardium. *J. Muscle Res. Cell Motil.* 34:295–310.
53. Ly, S., and S. S. Lehrer. 2012. Long-range effects of familial hypertrophic cardiomyopathy mutations E180G and D175N on the properties of tropomyosin. *Biochemistry.* 51:6413–6420.
54. Janco, M., A. Kalyva, ..., M. A. Geeves. 2012.  $\alpha$ -Tropomyosin with a D175N or E180G mutation in only one chain differs from tropomyosin with mutations in both chains. *Biochemistry.* 51:9880–9890.